Int J Adv Manuf Technol (2013) 69:1009–1016
DOI 10.1007/s00170-013-5108-5

ORIGINAL ARTICLE

A mixed elastohydrodynamic lubrication model with layered elastic theory for simulation of chemical mechanical polishing

Ping Zhou · Dongming Guo · Renke Kang · Zhuji Jin

Received: 10 October 2012 / Accepted: 29 May 2013 / Published online: 9 June 2013

Abstract Mixed elastohydrodynamic lubrication (mixed EHL) model has been successfully used to study phenomena in chemical mechanical polishing (CMP) process. However, in various mixed EHL simulation frameworks, a polishing pad's deformation cannot correctly be described by adopted models for pad deformation such as elastic half-space model and Winkler elastic foundation model. Thus, a more accurate model for pad deformation is needed, since this is the prerequisite for an accurate prediction of contact pressure and material removal rate, which is critical for improvement of polishing quality. In this paper, a layered elastic theory, which is frequently used to calculate flexible pavement response to truck loading, is introduced into the mixed EHL model. It is found that this theory has a similar accuracy to the traditional 3D finite element method for calculating the pad deformation. However, its computational cost is much lower, which is especially important for accurate and efficient simulation of mechanical behavior and material removal rate (MRR) in CMP. In order to highlight benefits of the proposed theory, simulations are carried out based on three different pad deformation models with the mixed EHL model. The pad deformation behavior is found to have a significant influence on the final simulation results, especially the MRR prediction. By comparing the different simulation models, the proposed layer elastic theory is found to be an optimal model for describing the polishing pad deformation behavior in CMP and can provide accurate simulation results on contact pressure distribution and the material removal rate.

Keywords Chemical mechanical polishing · Elastohydrodynamic lubrication · Layered elastic theory · Wafer · Material removal rate

P. Zhou (✉) · D. Guo · R. Kang · Z. Jin
Key Laboratory for Precision and Non-Traditional Machining Technology of Ministry of Education, Dalian University of Technology, Dalian 116024, China
e-mail: pzhou@dlut.edu.cn

1 Introduction

Chemical mechanical polishing (CMP) is extensively used to obtain a flat and smooth surface [1] in the manufacturing of integrated circuit (IC) chips, smart devices, and MEMS/NEMS. With progressively decreasing IC feature size, circuit wire is becoming much thinner and more fragile. For fabrication of IC chips in a decreased feature size, the substrate must have a flatter and smoother surface. Such a substrate is also strongly needed in fabricating smart devices and MEMS/NEMS components, in which an ultraflat surface with a flatness of about 1 nm [2, 3] is the prerequisite for bonding two separated substrates by intermolecular forces. Thus, as the only local/global planarization technique accepted by the IC industry, CMP's machining capability should be further improved to meet the needs of the IC industry.

In a typical CMP setup, as shown in Fig. 1, a wafer rotating around its axis is held by a carrier and pressed against a polishing pad with supply of polishing slurry. Material removal is realized by a combination of chemical reactions and mechanical abrasion induced, respectively, by chemicals and nanosized abrasive particles in the slurry. Moreover, the material removal is greatly affected by processing parameters and related physical parameters, like rotational speeds of the wafer and table, total downward pressure on wafer, elastic modulus of the pad, surface morphology of the pad, etc. These factors also obviously affect final polishing quality and efficiency, especially surface roughness, material removal rate, and within-wafer nonuniformity (WIWNU). Over the last two decades, in spite of great breakthroughs in CMP, many problems are still not clearly illustrated, such as slurry flow field, contact pressure distribution, evolution of the wafer's surface profile in CMP process, etc. To achieve ultrasmooth and ultraflat surface with high efficiency, there is a need for a better understanding of the physical and chemical phenomena in CMP, and an accurate simulation method will be greatly helpful in optimizing the CMP process.

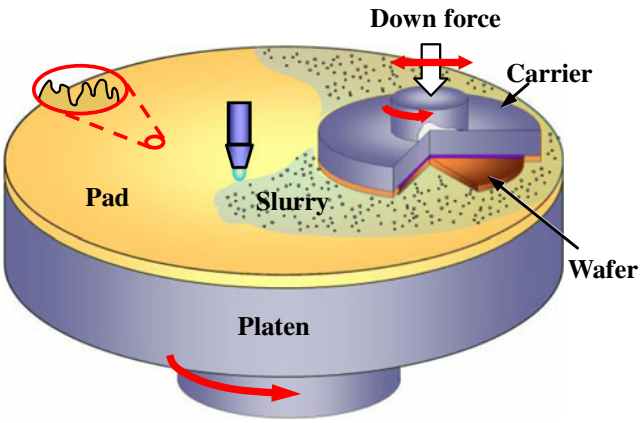

Fig. 1 Schematic diagram of the CMP system

From the physical perspective, the slurry flow and contact pressure distribution at the pad/wafer interface is highly related with the edge roll-off effect, which significantly affects lithography focus control at the peripheral region of the wafer. In order to increase the number of dies on a wafer, shrinkage at the edge induced by edge roll-off should be reduced [4]. Contact pressure at pad/wafer interface is very useful for analyzing the wafer edge roll-off [5]. Numerous researches have been focused on this topic, and most of them are based on the axisymmetric elastic solid model with finite element method (FEM) [5–7]. Although the length of wafer edge roll-off can be qualitatively explained by these models, a basic assumption in these models is that the deformation is axisymmetric, which is inconsistent with the actual situation due to the oblique orientation of the wafer in CMP process. Another shortcoming of these axisymmetric elastic solid models is that it cannot simulate the interaction between lubrication and wear that is, respectively, caused by the slurry and solid contact. Thus, it is impossible to correctly predict the maximum contact pressure, which is very important to predict the failure of Cu/ultralow k interconnections during polishing of the IC chip substrate. Also, a correct simulation of contact pressure is of critical importance for predicting the material removal rate.

Compared with the axisymmetric FEM CMP model, a more reasonable and practical simulation framework of CMP process is generally based on the tribology theory. Different from common tribological applications in which friction and wear needs to be reduced, a certain friction and wear is needed to realize material removal in CMP, in which the interaction between wear and lubrication has been investigated by many researchers. For the mixed lubrication behavior in CMP, the most classical simulation framework is developed by Kim et al. [8], which considers the deformation of the pad and the contact behavior between asperities and wafer. In order to predict the pad deformation, there are mainly three kinds of models used about mixed EHL model of CMP: (1) Winkler elastic foundation model [8, 9], (2) elastic half-space model [10–12], and (3) 3D finite element analysis [13]. In the Winkler elastic foundation model, also called "mattress" model or spring bed model, the polishing pad is modeled as a series of independent springs with no lateral interaction with each other. It is helpful to simplify the problem, but the analysis error is larger under a larger pad thickness especially at the wafer periphery. Different from the Winkler model, in elastic half-space model, the polishing pad thickness is assumed to be infinity, due to which the pad deformation is often overevaluated. As for the 3D FEM, it is indeed a reliable and robust method for assessing the pad deformation. However, due to the polishing pad's high aspect ratio, numerous discrete 3D elements and nodes are needed for FEM analysis, which will lead to very high computational cost, and it is not suitable as an iterative calculation step in the mixed EHL analysis.

In this paper, a layered elastic theory, frequently used in calculating the deformation of flexible pavement in response to the truck loading, is introduced into the mixed EHL for analyzing the pad deformation with similar accuracy, but higher efficiency, than the 3D FEM method. The simulation results from different pad deformation models are compared and analyzed, and a method for predicting the MRR based on the Preston equation is proposed. Also, the MRR distributions are calculated based on the contact pressure distributions obtained, respectively, from three different simulation methods.

2 Framework of simulation

The distributions of the contact pressure and slurry pressure are both dominated by the separation between wafer and pad surface, which is affected by the bulk deformation of pad. The pad deformation, in turn, is influenced by the contact pressure and slurry pressure. Therefore, the slurry flow and solid contact in CMP process are highly coupled. The framework for CMP simulation presented here is similar to that proposed by Jin et al. [9]. The key distinctions are that,

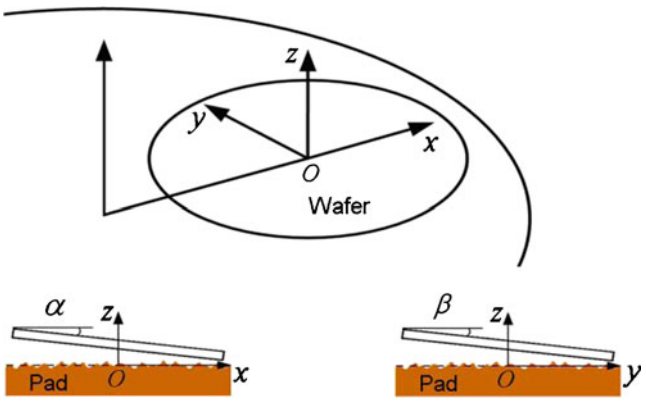

Fig. 2 Coordinate system defined in the CMP model

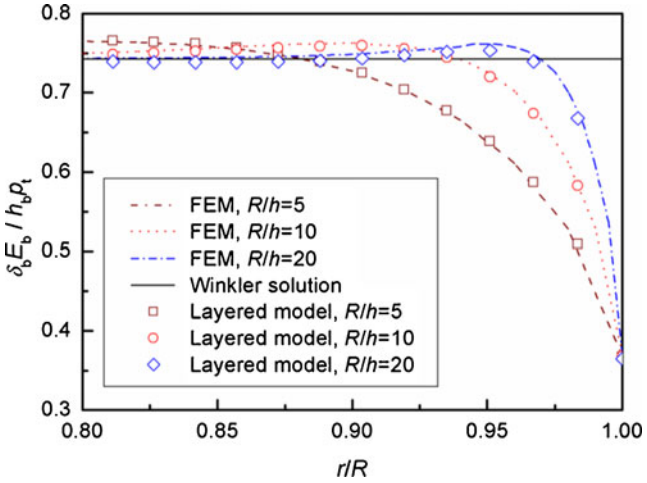

Fig. 3 Verification of the layered model with various values of R/h

firstly, the Winkler model is replaced by a layered elastic theory or elastic half-space model and, secondly, surface roughness and asperity deformation's effect on the slurry flow is considered.

2.1 Formulation of contact problem of layered elastic body

The polishing pad used in CMP is a typical layered elastic body, with a thickness of several millimeters and a diameter of several hundred millimeters. The normal deformation, $w(r)$, due to a concentrated load, P, on the surface of a layered elastic body is known as the generalized Boussinesq solution and can be given in terms of the Hankel transform [14, 15]:

$$w(r) = \frac{P\left(1-\upsilon_b^2\right)}{\pi E_b} \int_0^\infty F_0(\xi h_b) J_0(\xi r) d\xi \tag{1}$$

where υ_b and E_b, respectively, denote Poisson's ratio and Young's modulus of the elastic layer, h_b is the thickness of the elastic layer, and $F_0(\xi h_b)$ is given as:

$$F_0(\xi h_b) = \frac{1 + 4\kappa\xi h_b e^{-2\xi h_b} - \kappa\lambda e^{-4\xi h_b}}{1-\left(\lambda + \kappa + 4\kappa\xi^2 h_b^2\right)e^{-2\xi h_b} + \kappa\lambda e^{-4\xi h_b}} \tag{2}$$

where κ and λ are functions of Poisson ratios of the elastic layer and the substrate. In the CMP system, compared with the soft pad material, the base of the metallic rotary can be regarded as a rigid body in the pad deformation analysis. In this case, $\lambda=\kappa^{-1}$, and the following equation can be acquired from Eq. (2) :

$$F_0(\xi h_b) = \frac{1 + 4\kappa\xi h_b e^{-2\xi h_b} - e^{-4\xi h_b}}{1-\left(\kappa^{-1} + \kappa + 4\kappa\xi^2 h_b^2\right)e^{-2\xi h_b} + e^{-4\xi h_b}} \tag{3}$$

where $\kappa=-1/(3-4\nu_b)$. $J_0(\xi h_b)$ in Eq. (1) is Bessel function and given as:

$$J_0(\xi r) = \frac{2}{\pi} \int_0^{\pi/2} cos(\xi r sin\tau) d\tau. \tag{4}$$

In CMP process, a distributed total pressure $p_t(x, y)$ (resultant pressure of the contact pressure $p_a(x, y)$ and the slurry pressure $p_l(x, y)$) is acted on the layered pad, and the corresponding surface deformation $\delta_b(x, y)$ can be derived by linear superposition as follows:

$$\delta_b(x,y) = \frac{\left(1-\upsilon_b^2\right)}{\pi E_b} \iint_\Omega p_t\left(x', y'\right) \left(\int_0^\infty F_0(\xi h_b) J_0(\xi\rho) d\xi \right) dx' dy' \tag{5}$$

where $\rho=[(x-x')^2+(y-y')^2]^{1/2}$.

The simulating region is discretized into a series of small triangular elements, thus using Gaussian integration, and Eq. (5) is then discretized into a matrix equation as:

$$\delta_b(x_i, y_i) = \sum_{j=1}^{N_n} F_{ij} p_t\left(x_j, y_j\right), \quad i = 1, 2, \ldots, N_n \tag{6}$$

where N_n is the total number of discrete nodes in the simulating region, (x_i, y_i) is the coordinates of node i. F_{ij} are denoted as the "flexibility coefficients" and represent the normal displacements of node i due to a unit normal pressure located at node j. From Eq. (5), F_{ij} is given as:

$$F_{ij} = \frac{\left(1-\upsilon^2\right)}{\pi E} \sum_{k=1}^{N_e} \iint_{\Omega_e} N_k^j\left(x', y'\right) \left(\int_0^\infty F_0(\xi h_b) J_0\left(\xi\rho\left(x', y'\right)\right) d\xi \right) dx' dy' \tag{7}$$

where $\rho=[(x_i-x')^2+(y_i-y')^2]^{1/2}$ and N_k^j is the interpolation function of node j in the kth element.

In order to demonstrate the advantages of the proposed model, the results from this model will be compared with those obtained from the Winkler foundation model and the

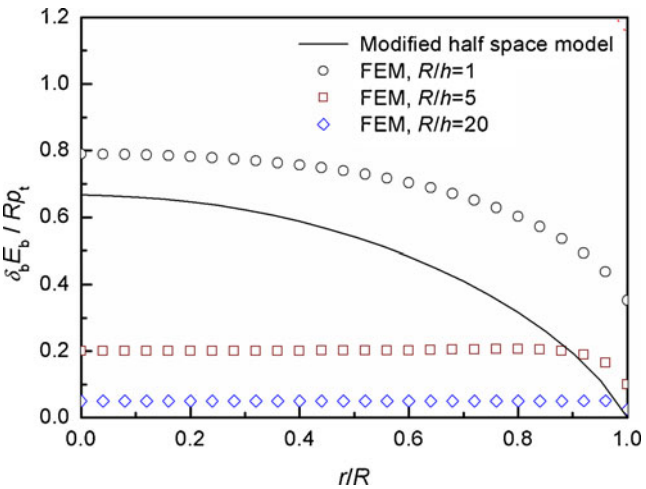

Fig. 4 Comparison between the results from FEM and the modified half-space model

elastic half-space model. In the Winkler foundation model, under the plane strain assumption, the formula describing the pad deformation mechanism is given as:

$$\delta_b(x_i,y_i)=\frac{p_t(x_i,y_i)}{k_b}=\frac{h_b(1-2\nu_b)(1+\nu_b)}{E_b(1-\nu_b)}p_t(x_i,y_i) \tag{8}$$

The above equation implies that the pad deformation is linearly proportional to the thickness of the pad. As for the elastic half-space model, the formula for obtaining pad deformation is given as:

$$\delta_b(x,y)=\frac{\left(1-\upsilon_b^2\right)}{\pi E_b}\iint_{\Omega}\frac{p_t\left(x',y'\right)}{\rho}dx'dy' \tag{9}$$

In elastic half-space model, the deformation is independent of the pad thickness. Consequently, the pad deformation is extremely overestimated. The researchers who adopted the elastic half-space model in 2D mixed EHL model of CMP process often modify the elastic half-space model based on an arbitrary assumption that the substrate deformation is zero at the leading edge [10–12]. Thus, a modified substrate deformation can be acquired:

$$\delta_b(x,y)=\frac{\left(1-\upsilon_b^2\right)}{\pi E_b}\iint_{\Omega}\frac{p_t\left(x',y'\right)}{\rho}dx'dy'-\delta_b(0,-R_w) \tag{10}$$

where R_w is the radius of wafer. In the 3D model proposed in this paper, the minimum deformation at the wafer boundary is assumed to be 0.

2.2 Simulation of mixed EHL behavior in CMP process

Since the fraction of abrasive in slurry is very small, the slurry can be approximately treated as a Newton fluid. The Reynolds formula of Newton fluid is:

$$\begin{aligned}&\frac{\partial}{\partial x}\left(\frac{\phi_p h^3}{12\mu}\frac{\partial p_l}{\partial x}\right)+\frac{\partial}{\partial y}\left(\frac{\phi_p h^3}{12\mu}\frac{\partial p_l}{\partial y}\right)=\\&\frac{\partial}{\partial x}\left(\overline{h}_T\frac{\boldsymbol{U}_w+\boldsymbol{U}_p}{2}\right)+\frac{\partial}{\partial y}\left(\overline{h}_T\frac{\boldsymbol{U}_w+\boldsymbol{U}_p}{2}\right)+\\&\frac{\partial}{\partial x}\left(\sigma\phi_s\frac{\boldsymbol{U}_p-\boldsymbol{U}_w}{2}\right)+\frac{\partial}{\partial y}\left(\sigma\phi_s\frac{\boldsymbol{U}_p-\boldsymbol{U}_w}{2}\right)+\frac{\partial\overline{h}_T}{\partial t}\end{aligned} \tag{11}$$

where μ is the dynamic viscosity of the slurry, σ is the standard deviation of distribution for the polishing pad's surface profile, p_l is the slurry pressure, h is the nominal film thickness, t is the time, h_T is the real film thickness, and $\overline{h}_T$ is the mathematical expectation of h_T. In hydrodynamic lubrication, i.e., wafer and pad are completely separated, $\overline{h}_T=h$. ϕ_p and ϕ_s in Eq. (5) are the pressure flow factor and the shear flow factor, respectively, which reflect surface roughness's influence on the slurry flow. $\boldsymbol{U}_w$ and $\boldsymbol{U}_p$ are the velocity vectors of the wafer and the polishing pad, respectively, given as:

$$\begin{aligned}\boldsymbol{U}_w&=\begin{pmatrix}U_w^x\\U_w^y\end{pmatrix}=\begin{pmatrix}-r\omega_w sin\theta\\r\omega_w cos\theta\end{pmatrix}\\\boldsymbol{U}_p&=\begin{pmatrix}U_p^x\\U_p^y\end{pmatrix}=\begin{pmatrix}-r\omega_p sin\theta\\r\omega_p cos\theta+d_e\omega_p\end{pmatrix}\end{aligned} \tag{12}$$

where ω is the rotation velocity; the subscripts w and p denote the wafer and the pad, respectively; θ is the angular coordinate of the calculation point, the origin of the cylindrical coordinate system is placed at the center of the wafer; and d_e is the distance between wafer center and platen center (or pad center).

The pressure flow factor in Eq. (11) can be given as that in [16]:

$$\phi_p=1-0.9\exp(-0.56H) \tag{13}$$

where the dimensionless nominal film thickness, H, is defined as h/σ_o. The shear flow factor in Eq. (11) can be given as [16]:

$$\phi_s=\begin{cases}1.899H^{0.98}\exp\left(-0.92H+0.05H^2\right) & H\le 5\\1.126\exp(-0.25H) & H>5\end{cases} \tag{14}$$

The average value of real film thickness is given as:

$$\overline{h}_T=\begin{cases}h & ,\quad H\ge 3\\3\sigma-\sigma\int_H^3\phi_c dH & ,\quad H<3\end{cases}. \tag{15}$$

The contact factor, ϕ_c, is defined by Wu and Zheng [17] as:

$$\begin{aligned}\phi_c&=\frac{\partial\overline{h}_T}{\partial h}\\&=exp\left(-0.6912+0.782H-0.304H^2+0.0401H^3\right).\end{aligned} \tag{16}$$

The nominal film thickness is related to the wafer orientation and the pad deformation. Defining the rotational angles around the x and y axes, respectively, as α and β as shown in Fig. 2, the nominal film thickness is obtained as:

$$h(x,y)=h_0-\alpha x-\beta y+\delta_b(x,y) \tag{17}$$

where h_0 is the height of wafer center and δ_b is the pad deformation in bulk. The compression deformation of the asperity is:

$$\delta_a(x,y)=h_{ini}-h(x,y) \tag{18}$$

where h_{ini} is the reference thickness, in which the deformation of asperities is 0. Adopting the GW model, the average contact pressure acting on the asperities is:

$$p_a=\frac{4E_a}{3\left(1-\nu_a^2\right)}\eta\sqrt{R_a}\int_h^{h_{ini}}(z-h)^{1.5}\varphi_a(z)dz \tag{19}$$

Table 1 Parameters used in the simulation example

Parameters		Value	Units	Parameters		Value	Units
Wafer	D_w	100	mm	Asperity	E_b	30	MPa
	d_e	100	mm		υ_b	0.49	
	h_v	5	mm		η	100	mm^{-2}
Pad in bulk	E_b	10	MPa		R_a	50	μm
	υ_b	0.3			σ	8	μm
	h_b	3	mm	Fluid	μ	0.001	Pa s
Rotation speed	ω_w	60	r min^{-1}	Friction coefficient	F	0.5	
	ω_p	60	r min^{-1}	Average pressure	p_{ave}	3	psi

where E_a and υ_a, respectively, denote the elastic modulus and Poisson's ratio, and η is the density of the asperities. The distribution of asperity peak heights is assumed to be a "clipped" exponential given as [8]:

$$\varphi_a(z) = \frac{1}{s}\frac{exp\left(-\frac{z}{s}\right)}{exp\left(-\frac{z_0}{s}\right)-exp\left(-\frac{z_{max}}{s}\right)} \tag{20}$$

where s is the average asperity height and the asperity height ranges from z_0 to z_{max}. In the present study, $s=\sigma$, $z_0=0$, and $z_{max}=4\sigma$. Eq. (20) satisfies:

$$\int_{z_0}^{z_{max}} \varphi_a(z)dz = 1. \tag{21}$$

The deformation of pad in bulk is calculated by Eq. (6).

In order to obtain the wafer orientation in the equilibrium condition, the resultant force and moments are needed to be calculated. The resultant force in the z direction acted on the wafer is:

$$F_z = \iint_{\Omega} p_t(x,y)dxdy. \tag{22}$$

The resultant moment around x or y axis are:

$$\begin{aligned} M_x &= \iint_{\Omega}\left[p_t y + f p_a h_v \frac{U_p^y - U_w^y}{|\boldsymbol{U}_p - \boldsymbol{U}_w|}\right]dxdy \\ M_y &= \iint_{\Omega}\left[-p_t x + f p_a h_v \frac{U_p^x - U_w^x}{|\boldsymbol{U}_p - \boldsymbol{U}_w|}\right]dxdy \end{aligned} \tag{23}$$

where f is the friction coefficient between asperities and the wafer, and h_v is the distance from the center of carrier's gimbal joint ball to the wafer surface.

2.3 Calculation of the MRR distribution

After carrying out the simulation of the mixed EHL behavior in CMP process, distribution of the nominal contact pressure will be obtained and then the MRR distribution can be calculate based on the Preston equation as:

$$\text{MRR} = kPV \tag{24}$$

where P is the nominal contact pressure and V is the relative shear velocity between the wafer and the polishing pad, which can be calculated based on Eq. (12):

$$V = \left(\left(r\omega_p sin\theta - r\omega_w sin\theta\right)^2 + \left(r\omega_p cos\theta + d_e\omega_p - r\omega_w cos\theta\right)^2\right)^{0.5}. \tag{25}$$

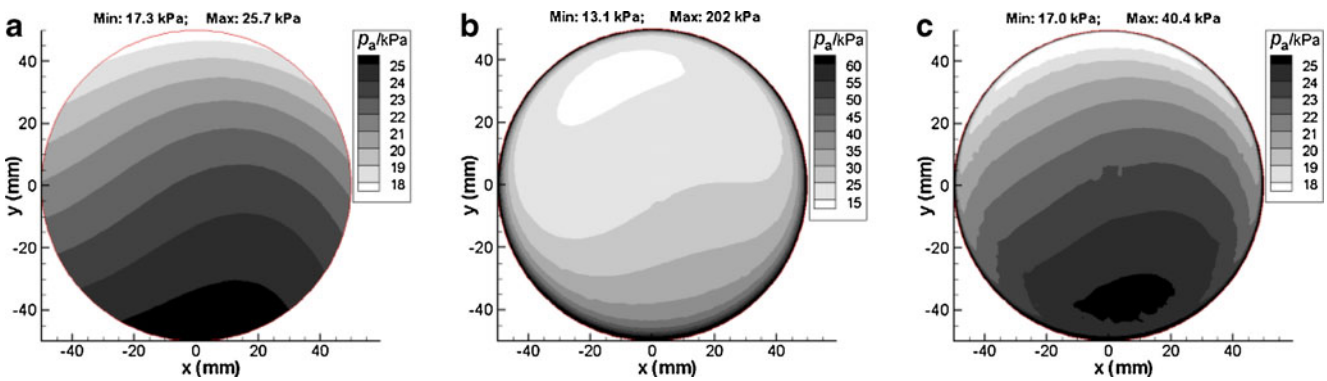

Fig. 5 Simulation results on the contact pressure distributions obtained from **a** EHL-W, **b** EHL-H, and **c** EHL-L, respectively

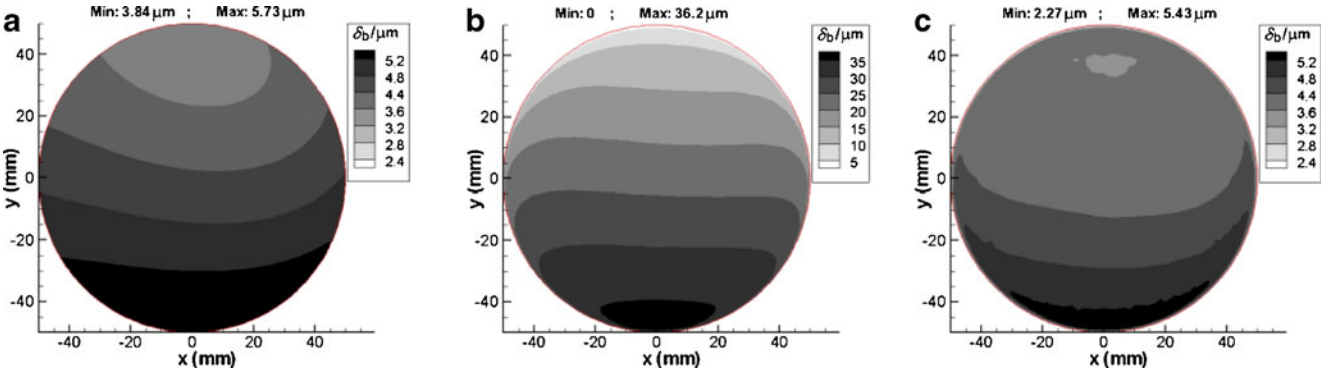

Fig. 6 Simulation results on the pad deformation obtained from **a** EHL-W, **b** EHL-H, and **c** EHL-L, respectively

Although the contact pressure distribution is not axisymmetric, the MRR distribution is axisymmetric due to the rotation of the wafer, i.e., the value of MRR will be the same at locations of the same r coordinate. The mean value of the product of the contact pressure and the relative shear velocity at points of the same r coordinate, but different θ coordinate, is used to evaluate the MRR.

3 Results and discussion

3.1 Verification of the pad deformation model

Simulation of the mixed EHL behavior is realized using the code written in FORTRAN language. In order to verify the code and the layered pad deformation model, numerical solutions of the pad deformation under uniform load based on Eq. (6) is compared with that from the axisymmetric FEM model. Also, a Winkler solution is also provided for comparison. From Fig. 3, it can be seen that the results obtained from Eq. (6) agree very well with those obtained with FEM, while the Winkler foundation model cannot correctly calculate the deformation around the wafer–pad contact edge. The prediction error from the Winkler foundation model increases with the decrease of R/h. By comparing the results from FEM method and the layered model, the layered elastic theory is verified to have nearly the same accuracy with FEM model in predicting the pad deformation and the contact pressure at the wafer periphery. Also, the comparison between from FEM and the modified half-space model is also showed in Fig. 4, from which it is found that the pad deformation cannot be correctly predicted by the elastic half-space model, since the pad deformation is assumed to be independent of the pad thickness in the half-space model, which is obviously inconsistent with the actual situation.

In the analysis of pad deformation, in-plane dimensions are considerably larger than the thickness dimension, but for higher calculation accuracy, the aspect ratio of the 3D solid element should be close to 1. Consequently, the number of the nodes used in the 3D finite element model is several times larger than that used in the layered elastic model. Moreover, the degrees of freedom (DOF) for the node used in 3D FEM and the layered elastic model are 3 and 1, respectively. Thus, the layered elastic method is more efficient to solve the pad deformation compared with the 3D finite element method.

Table 2 Wafer positions and orientations in the equilibrium condition

Models	h_0 (μm)	α (μrad)	β (μrad)
EHL-W	16.3	2.18	−33.0
EHL-H	−2.67	5.83	−338
EHL-L	16.6	2.20	−31.8

3.2 Simulation results of mixed EHL behaviors in CMP

To highlight the significance of the layered elastic theory, simulation results from the Winkler foundation model (EHL-W), the modified half-space model (EHL-H), and the newly proposed layered elastic theory (EHL-L) are compared. In the 2D EHL-H model, the pad deformation is assumed to be zero at the leading edge [10–12], while for the 3D EHL-H model, the maximum pad deformation at the wafer's boundary is set to be zero. This assumption will not affect the slurry film thickness and the contact pressure distribution, but the prediction of the pad deformation will be affected. The parameters used in the simulation are shown in Table 1.

The simulation results from the three different models on the contact pressure distribution at wafer/pad interface are showed in Fig. 5, from which it can be seen that the patterns of the obtained pressure distributions are different. As for the pressure distribution, the distribution predicted by EHL-H is different from that predicted by EHL-W or EHL-L. EHL-W and EHL-L have similar simulation results in the central area of the wafer, but the predicted pressure distributions are obviously different at the periphery. Since the contact pressure is dominated by the gap thickness between the wafer

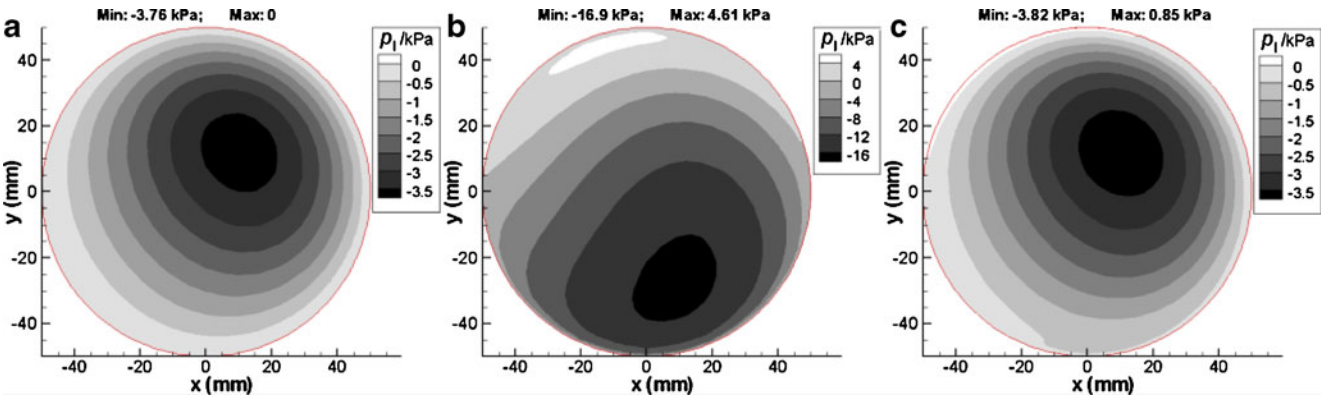

Fig. 7 Simulation results on the slurry pressure distribution obtained from **a** EHL-W, **b** EHL-H, and **c** EHL-L, respectively

surface and pad surface, the sudden decrease in gap thickness at wafer's periphery will lead to increased contact pressure in this region. From this perspective, the simulation result from EHL-L is obviously much closer to the real situation. Another factor that can be used to evaluate effectiveness of these three models is the stress concentration effect. Based on the theory of contact mechanics, when a rigid surface is pressed against a soft surface, stress concentration will occur at the contact boundary. By comparing the simulation results in Fig. 5, it can be seen that the stress concentration effect can be predicted both by EHL-H and EHL-L models, but not by EHL-W. As for EHL-H and EHL-L, although the stress concentration can be predicted by the EHL-H model, due to the incorrect prediction of pad deformation as shown in Fig. 4, the simulation results on contact pressure distribution from the EHL-H model is of no significant practical value. Based on the above two points, among the three models, the EHL-L model is more accurate in predicting the pressure distribution. A correct prediction of maximum contact pressure is very important for estimating the possibility of the surface damage in CMP process. In the simulation result obtained from EHL-L (Fig. 5c), the stress concentration occurs mainly within a distance of about 5 mm from the wafer boundary, which can be used for correct analysis of edge roll-off.

Along with the pressure distribution, the pad deformation can also be obtained, as showed in Fig. 6. Similar to the situation in predicting the pressure distribution, EHL-W and EHL-L have similar simulation results, which are significantly different than that obtained from EHL-H. As for the magnitude of the pad deformation, the values from EHL-W and EHL-H are about 2–6 μm, which value from EHL-H is about 0–37 μm. Different pad deformation behaviors predicted from the three models will induce different wafer equilibrium positions and orientations. As showed in Table 2, the wafer equilibrium positions and orientations by the EHL-H model are significantly different with those by EHL-W and EHL-L models. Besides, different pad deformations predicted by these three models will lead to different slurry pressure distributions. As shown in Fig. 7, the slurry pressure predicted by EHL-W is negative in the whole region beneath the wafer, but for the slurry pressure distributions obtained from EHL-H and EHL-L, there is a small region with positive slurry pressure in the whole contact area.

One of the important aims of numerical simulation of CMP process is to predict the distribution of MRR along the wafer radius, which is of significant importance to improve the global planarity. Based on the Preston equation, the MRR is linearly proportional to the product of the contact pressure and the relative shear velocity between the wafer and the pad. Figure 8 shows the average value of $P_a \cdot V$ along the radius obtained from the different simulation frameworks. It is found that although the axisymmetric FEM model can qualitatively predict the edge roll-off, the result is completely different from that obtained by EHL models and, thus, is not preferred for MRR prediction. Among the three mixed EHL models, the EHL-W model has similar MRR prediction ability to EHL-L model, except that the EHL-W cannot predict the edge roll-off as EHL-L does. Thus, the EHL-L model is the most accurate among these

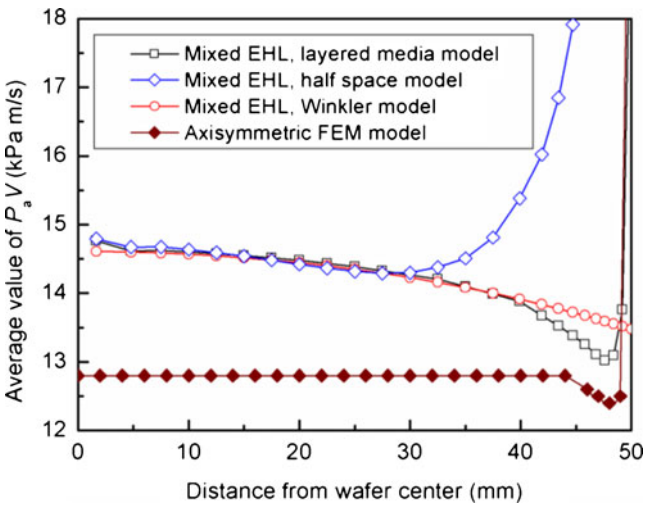

Fig. 8 Comparison of material removal rates based on different models

models for predicting MMR. However, when the edge roll-off is not highly concerned, the EHL-W model can be recommended for simulating of the CMP process due to its high calculation efficiency.

4 Conclusions

A new simulation framework for CMP process based on the layered elastic theory is proposed in this paper. The layered elastic theory, with similar accuracy with FEM, is convenient to be used in the simulation framework of mixed lubrication behavior in the CMP process. Simulation results from different pad deformation models are compared. From the perspectives of contact pressure distribution pattern, stress concentration effect at the wafer periphery, and also the edge roll-off effect, the layered media model is found to be the most accurate model for predicting the contact pressure at the wafer periphery, which is very important to analyze the edge roll-off value and maximum contact pressure exerted on the wafer surface. However, when the edge roll-off is not highly concerned, the EHL-W model is still the best choice for simulating the CMP process because of its high efficiency. Another problem that needs to be pointed out is that although the Boussinesq solution is a good choice to replace the 3D FEM solution on a uniform elastic pad, the 3D FEM solution still has more general applications, especially in the situations where the pad contains features such as grooves or holes, or the pad thickness is nonuniform due to dressing or conditioning.

Cross-checking between the simulation results and the experiment data is a simple and intuitive way to validate the effectiveness of the simulation framework. However, in same situations, it is difficult to carry out the experiment to verify the fine distinctions between the simulation results obtained from different simulation frameworks, like the stress concentration at wafer periphery. Since there are many steps and models in the simulation framework of CMP, a more convincing and effective validation method is to check the models used in each step. As for the problem of CMP simulation framework discussed in this paper, a correct simulation of pad deformation has been carried out and validated in this paper, and the slurry flow model and asperity contact model will be validated in our future work.

Acknowledgments The authors would like to acknowledge the support of the National Natural Science Foundation of China (51105057, 91023043) and China Postdoctoral Science Foundation (201104598). The idea of this method was first reported at the International Symposium on Advances in Abrasive Technology (ISAAT) XV in Singapore in 2012 [18]. The authors thank Trans Tech Publications Ltd. for their permission to publish an extended version in another periodical. The authors also would like to thank Dr. Zhe Li from the National University of Singapore for his assistance in language editing.

References

1. Kasai T, Bhushan B (2008) Physics and tribology of chemical mechanical planarization. J Phys Condens Matter 20(22):1–13. doi:10.1088/0953-8984/20/22/225011
2. Ogihara M, Sagimori T, Mutoh M, Furuta H, Suzuki T, Fujiwara H, Sakuta M (2008) Single crystal thin film bonding on diamond like carbon film by intermolecular force for super high-density integration of high-power LEDs. In: 2008 I.E. international electron devices meeting, San Francisco, CA, USA, pp 1–4. doi:10.1109/IEDM.2008.4796729
3. Kirino O, Enomoto T (2011) Ultra-flat and ultra-smooth Cu surfaces produced by abrasive-free chemical–mechanical planarization/polishing using vacuum ultraviolet light. Precis Eng 35(4):669–676. doi:10.1016/j.precisioneng.2011.05.005
4. Li Y (2007) Microelectronic applications of chemical mechanical planarization. Wiley, New York, p 408
5. Chen KS, Yeh HM, Yan JL, Chen YT (2009) Finite-element analysis on wafer-level CMP contact stress: reinvestigated issues and the effects of selected process parameters. Int J Adv Manuf Technol 42(11):1118–1130. doi:10.1007/s00170-008-1672-5
6. Lee H, Jeong H (2011) A wafer-scale material removal rate profile model for copper chemical mechanical planarization. Int J Mach Tools Manuf 51(5):395–403. doi:10.1016/j.ijmachtools.2011.01.007
7. Lo SP, Lin YY, Huang JC (2007) Analysis of retaining ring using finite element simulation in chemical mechanical polishing process. Int J Adv Manuf Technol 34(5–6):547–555. doi:10.1007/s00170-006-0622-3
8. Kim AT, Seok J, Tichy JA, Cale TS (2003) Soft elastohydrodynamic lubrication with roughness. J. Tribol Trans ASME 125(2):448–451. doi:10.1115/1.1494100
9. Jin X, Keer LM, Wang Q (2005) A 3D EHL simulation of CMP. J Electrochem Soc 152(1):7–15. doi:10.1149/1.1823993
10. Zhang ZH, Du YP, Luo JB (2006) Analysis on contact and flow features in CMP process. Chin Sci Bull 51(16):1961–1965. doi:10.1007/s11434-006-2090-4
11. Tichy J, Levert JA, Shan L, Danyluk S (1999) Contact mechanics and lubrication hydrodynamics of chemical mechanical polishing. J Electrochem Soc 146(4):1523–1528. doi:10.1149/1.1391798
12. Hu I, Yang TS, Chen KS (2011) Synergistic effects of wafer rigidity and retaining-ring parameters on contact stress uniformity in chemical mechanical planarization. Int J Adv Manuf Technol 56:523–538. doi:10.1007/s00170-011-3215-8
13. Kim AT, Seok J, Tichy JA, Cale TS (2003) A multiscale elastohydrodynamic contact model for CMP. J Electrochem Soc 150(9):570–576. doi:10.1149/1.1598215
14. Burmister DM (1945) The general theory of stresses and displacements in layered soil systems. J Appl Phys 16(2):89–94. doi:10.1063/1.1707562
15. Muki R, Dong SB (1980) Elastostatic far-field behavior in a layered half space under surface pressure. J Appl Mech 47(3):504–512. doi:10.1115/1.3153723
16. Patir N, Cheng HS (1979) An application of average flow model to lubrication between rough sliding surfaces. J Lubr Technol 101(2):220–229. doi:10.1115/1.3453329
17. Wu CW, Zheng LQ (1989) An average Reynolds equation for partial film lubrication with a contact factor. ASME J Tribol 111(1):188–191. doi:10.1115/1.3261872
18. Zhou P, Kang RK, Jin ZJ, Guo DM (2012) Simulation of CMP process based on mixed elastohydrodynamic lubrication model with layered elastic theory. Adv Mater Res 565:330–335. doi:10.4028/www.scientific.net/AMR.565.330